Available online at www.sciencedirect.com

ScienceDirect

Physics Procedia 52 (2014) 80 – 89

Physics Procedia

Physics and Applications of High Brightness Beams Workshop, HBEB 2013

Compression of a 20 pC e-bunch at the European XFEL for Single Spike Operation

B. Marchetti[a,*], M. Krasilnikov[a], F. Stephan[a], I. Zagorodnov[b]

[a] *DESY, Platanenallee 6, Zeuthen 15738, Germany*
[b] *DESY, Notkestrasse 85, Hamburg 22607, Germany*

Abstract

The production of ultra-short (fs or sub-fs long), high power, radiation pulses in the x-ray spectral region, represents a challenge for many existent SASE FELs.
In order to realize single spike lasing the length of the electron bunch must be extremely small (less than a micrometer) thus it is necessary to tune the linac and magnetic chicanes near to the maximum compression point. In this setup, the final length of the electron bunch strongly depends on the non-linearity of its longitudinal phase space. The use of a third harmonic RF cavity section placed right after the injector is foreseen at the European XFEL in order to correct the longitudinal phase space non-linearity up to the third order.
We describe a method for the optimization of the electron bunch compression presenting beam dynamics simulations for a 20 pC electron bunch.

Peer-review under responsibility of the scientific committee of HBEB 2013

Keywords: SASE; longitudinal coherence; European XFEL; bunch compression; short x-ray pulses

1. Introduction

There is a considerable interest within the accelerator community in generating extremely short, fully longitudinally coherent x-ray pulses by Self Amplified Spontaneous Emission Free Electron Lasers (SASE FELs). The lower limit of the radiation pulse duration is mainly set by the shortest achievable length of the electron bunch at the entrance of the undulator, while the lack of longitudinal coherence comes from the fact that the final radiation pulse is obtained from the amplification of the spontaneous radiation. When the electron bunch enters the undulator many longitudinal modes are exited and spontaneous radiation at different wavelengths according to the electron energy is produced [Huang et al. 2007]. The SASE FEL process amplifies then all the frequency components within the acceptance bandwidth of the FEL. If we look at the longitudinal profile of the radiation pulse we observe that it is composed by many spikes (or modes) and the same number of spikes is present in the energy spectrum.

* Corresponding author. Tel.: +49 337627 7185.
E-mail address: barbara.marchetti@desy.de

Peer-review under responsibility of the scientific committee of HBEB 2013
doi:10.1016/j.phpro.2014.06.013

Many methods have been proposed in order to produce fully coherent and/or extremely short x-ray radiation pulses using FELs, not necessarily in the conventional SASE configuration.

The use of a seed allows to obtain a better longitudinal coherence of the radiation pulse. The lack of good seeds for FELs in the x-ray region led to the invention of the self-seeding scheme [Amann et al. 2012], originally proposed at DESY [Feldhaus et al. 1997]. The tapering technique may allow to obtain both longitudinally coherent and extremely short radiation pulses. This technique already allowed single spike lasing at longer wavelengths at the SPARC facility [Giannessi et al. 2011] [Marcus et al. 2012]. For x-ray lasing, the required strong energy modulation within a short slice of the electron bunch can be produced by a few-cycle optical laser pulse in a short undulator, placed in front of the main undulator [Saldin et al 2006]. The recently proposed mode-locked x-ray SASE FEL technique [Thompson et al. 2008] allows to obtain trains of attosecond x-ray pulses by interposing properly set chicanes between the undulators. The enhanced SASE technique allows to obtain trains of few-cycle x-ray pulses from a FEL amplifier via a so called afterburner, i.e. several few periods undulator sections separated by chicanes [Dunning et al. 2013].

If we do not want to introduce any change in the machine layout, the easiest scheme to be applied remains the optimization of the compression of low charged bunches [Reiche at al. 2008] [Rosenzweig et al. 2008]. Due to the present lack of diagnostics for very low charges, some efforts both on the theoretical and experimental side has been spent at LCLS on the optimization of the compression of a 20 pC charged bunch [Wang et al. 2011] [Ding et al. 2009].

In this paper we would like to extend the optimization of the compression of a 20 pC electron bunch to the European XFEL layout including also the comparison of the performances delivered by different setups of the photo-cathode laser. The motivation for this study is supplied by the observation that the experimental characterization of a new working point for short pulses operation at the European XFEL is already feasible at the PITZ facility [Stephan et al. 2010] [Krasilnikov et al. 2012].

1.1. Single spike condition

The radiation produced by SASE FELs is characterized by an energy spectrum constituted by many spikes. The number of the spikes depends on the longitudinal properties of the electron bunch. In fact, once the bunch is injected into the undulator, the radiation emitted by the electrons located in a certain longitudinal position can be amplified only by other electrons placed within a fixed longitudinal distance (in the forward direction) from them. This distance is proportional to the cooperation length, defined as a radiation slippage in one power gain length [Bonifacio et al. 1994]. The cooperation length L_c depends on the emitted radiation's wavelength λ, according to:

$$L_c = L_{c1d}\,(1 + \eta) \tag{1}$$

where the parameter η, defined as in [Boscolo et al. 2008], takes into account transverse effects and beam energy spread, and L_{c1d} is the one-dimensional cooperation length, defined as:

$$L_{c1d} = \frac{\lambda}{\sqrt{3}(4\pi\rho)} \tag{2}$$

with ρ being the one dimensional FEL parameter. Every longitudinal slice in the bunch whose length is $2\pi L_c$ contributes to a different spike in the energy spectrum of the produced radiation, thus in order to have a single spike, the electron bunch must be shorter than $2\pi L_c$. It is very difficult to satisfy this condition in x-ray FELs where, according to equations 1 and 2, $2\pi L_c$ becomes very small, typically a fraction of μm.

1.2. Motivation and procedure

In order to fulfill the single spike condition (or get as close as possible to it) the charge of the electron bunch must be small (sub pC or few tens of pC) and it is necessary to work at the maximum compression point (or very close to it). These two requirements make the working point deeply different from the nominal XFEL working point that has been already extensively studied [Zagorodnov et al. 2011] and that has to fulfill mainly the ultra-high brilliance request. The optimization of the injector setup of the nominal European XFEL working points has been carried out by minimizing the transverse emittance of the electron bunch. In [Zagorodnov et al. 2010] has been underlined that the use of a similar approach for the ultra-short low charge operation ends up into strong stability requirements for the RF

jitter. In order to relax the RF stability requirements at FLASH a new photo-cathode laser has been recently installed which allows for the generation of shorter electron bunches right at the cathode [Rehders et al. 2012]. The European XFEL facility is foreseen to have a unique type of photo-cathode laser, whose prototype is currently installed at PITZ [Will et al. 2008]. This laser allows to tune the longitudinal flat-top shape of the pulse up to 20ps FWHM. The shortest feasible laser profile is a Gaussian having a FWHM of about 2 ps. The nominal XFEL working point foresees a flat-top laser pulse of 20 ps length, but we are now going to discuss alternative laser parameters to be used for the short pulse operation [Marchetti et al. 2012]. In the present work we will analyze the optimization of the compression of a 20pC electron bunch for single spike operation in the hard x-rays (0.26 nm). As we have already mentioned, the choice of the bunch charge has been made after considering that the diagnostic foreseen at the European XFEL currently has a lower limit at 20 pC bunch charge. In our paper we have decided to vary the photo-cathode laser parameters looking for a setup that simultaneously relaxes the RF stability with respect to the voltage jitter and minimizes the achievable bunch length after the compression. The first aim can be reached by using short electron bunch distributions already at the gun exit. The second one deserves a longer discussion but we can anticipate that two factors play the most important role: the possibility to sufficiently correct the non-linear terms in the longitudinal phase space distribution and the slice energy spread of the electron bunch at the gun exit.

The change of the photo-cathode laser parameters to observe the consequences in the electron bunch distribution at the linac exit is a very delicate task. In every run indeed we need to re-decide the linacs and compressors setup in order to be able to compare the different results. This prevent us from the possibility of simply scanning the laser parameters, that is why we have limited our study to a few interesting cases.

2. Simulations

2.1. European XFEL layout

In Fig. 1 a scheme of the layout of the European XFEL is shown. The injector is composed by a photocathode RF gun (1.6 cell L-band normal conducting gun, having 60 MV/m peak Electric field at the Cs2Te cathode), a cryomodule with eight TESLA accelerating cavities having frequency of 1.3 GHz and a section of eight third harmonic cavities running at 3.9 GHz. Through the use of the third harmonic RF-cavity section, the correction of the non-linearity in the longitudinal phase space distribution of the electron bunch is possible. The laser heater (*LH*) can mitigate the effect of micro-bunching instability. The electron bunch compression starts in the dogleg (*DL*) and is completed in three magnetic stages (BC_s).

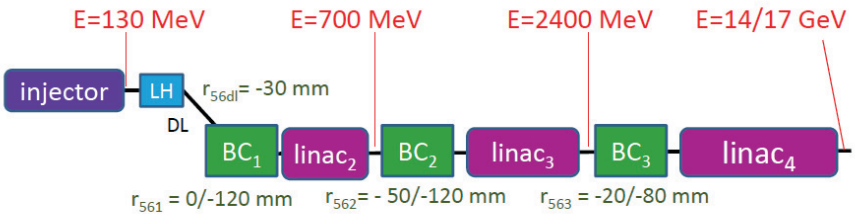

Fig. 1. Schematic layout of the European XFEL.

2.2. Input beams

The study has been restricted to two longitudinal laser shapes: a longitudinally gaussian pulse having 2.1 ps FWHM and a flat-top pulse having 5.4 ps FWHM and 2ps rise/fall time. The first distribution has been chosen since it is almost the shortest gaussian pulse feasible with the the PITZ/XFEL photo-cathode laser (we have preferred 2.1

ps to 2.0 ps, which is the actual limit, to be more conservative). The second distribution has been obtained by scaling the laser parameters of the XFEL working point for 1nC e-bunch to 20 pC keeping constant the produced charge density. Both the distributions have a flat-top transverse shape: the second one has 0.11 mm RMS, while for the longitudinally gaussian distribution three RMS spotsize values have been studied (0.1 mm, 0.07 mm and 0.064 mm). The longitudinal phase space distributions at the entrance of the first accelerating cavity of the injector for these 4 working points are represented in Fig. 2 (a). Moreover plots b and c compares the slice energy spread and the normalized slice emittance of such distributions respectively.

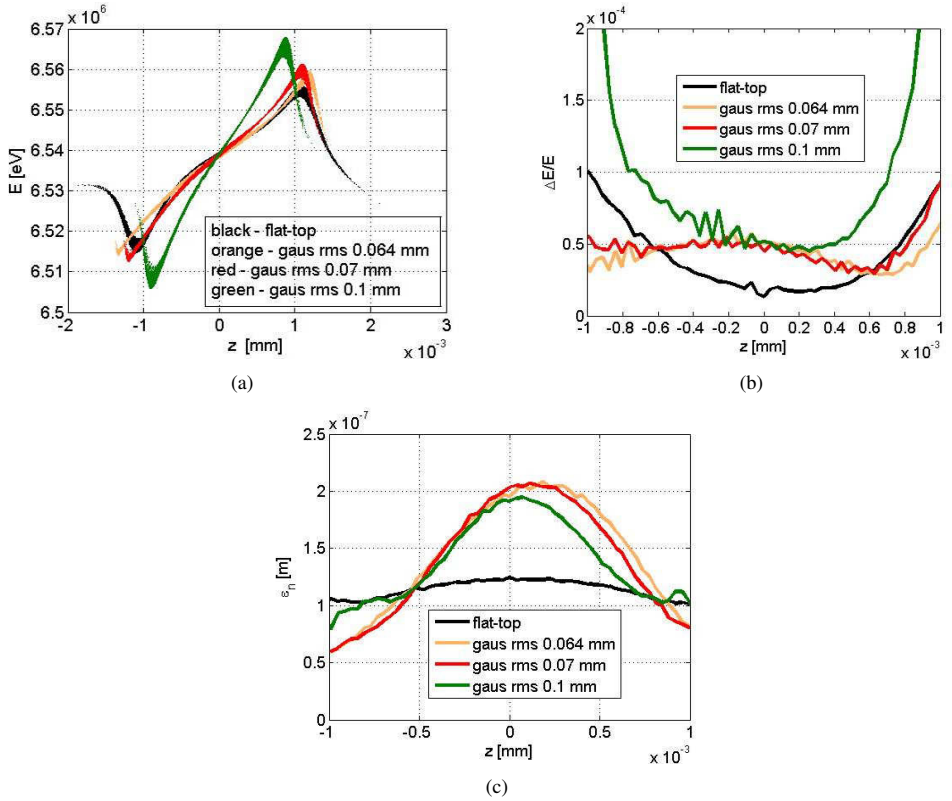

Fig. 2. Longitudinal phase space distribution (a), slice energy spread (b) and slice emittance (c) at 3 m from the cathode (i.e. just before the entrance in the first accelerating cavity) for the 4 input beams.

2.3. Injector setup and non-linearity correction procedure

The correction of the non-linearity in the longitudinal phase space is a critical point: in order to achieve the shortest bunch length at maximum compression the non-linearity present in the longitudinal phase space of the electron bunch at the gun exit must be precisely known and compensated.

The energy deviation distribution of the electron bunch $\delta(s)$ at the gun exit as a function of the longitudinal coordinate s can be expressed as:

$$\delta(s) \equiv \delta'(0)s + \frac{\delta''(0)}{2}s^2 + \frac{\delta'''(0)}{6}s^3 \tag{3}$$

For our study we don't need to change the setup of the main linac (i.e. voltages and phases for $linac_2$, $linac_3$ and $linac_4$ and the curvature radius of the BCs), thus these parameters have been fixed to reasonable values known from past studies.

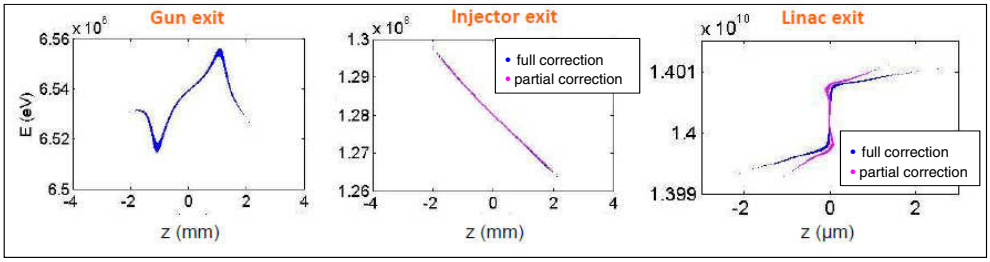

Fig. 3. Longitudinal phase space distributions at the gun exit (left) at the injector exit (middle) and at the linac exit (right). The distribution at the gun exit has been obtained by using the ASTRA code [Floettmann 2011]. This longitudinal phase space distribution has then been tracked along the linac using the matrix transport. The RF-wakefields have been added analytically. The blue distributions correspond to the optimal injector working point to have a "fully" (up to the third order) non-linearity correction. Unfortunately this setup uses extremely high voltages setpoints for the injector. In these first simulations we have imposed as maximum on crest voltages the values $V_{11} \leq 180$ MV and $V_{13} \leq 40$ MV. The pink distributions correspond to the best correction of non-linearity achievable if we keep the voltages in the injector below these maxima. The latter working point has been used in the start to end simulations.

At this point we wish to find one longitudinal phase space distribution $\delta_1(s)$ at the exit of the injector that will evolve into a linear distribution, at least in the central part of the beam, at the exit of $linac_3$. The distribution $\delta_1(s)$ is represented through its derivatives $\alpha_i = \frac{\partial^i \delta_1}{\partial s}(0)$, similarly to eq. 3.
By imposing the longitudinal matching condition, defined in [Floettmann et al. 2001], at the exit of the last bunch compressor and backtracking the solution up to the injector exit it is possible to calculate analytically a first guess of $\delta_1(s)$. Moreover the longitudinal phase space distribution $\delta(s)$ at the gun exit can be easily extracted from the output of an ASTRA [Floettmann 2011] simulation.

Thus the setup of the injector (voltages and phases of the RF cavities) that delivers the required phase space distribution $\delta_1(s)$ at its exit is uniquely determined by the equations

$$\begin{bmatrix} 1 & 0 & 1 & 0 \\ 0 & -k & 0 & -nk \\ -k^2 & 0 & -(nk)^2 & 0 \\ 0 & k^3 & 0 & (nk)^3 \end{bmatrix} \begin{bmatrix} X_{11} \\ Y_{11} \\ X_{1n} \\ Y_{1n} \end{bmatrix} = \begin{bmatrix} E_1^0 - E_0^0 \\ E_1^0 \alpha_1 - E_0^0 \delta'(0) \\ E_1^0 \alpha_2 - E_0^0 \delta''(0) \\ E_1^0 \alpha_3 - E_0^0 \delta'''(0) \end{bmatrix} \tag{4}$$

containing the variables

$$\begin{aligned} X_{11} + iY_{11} e^{i\phi_{11}} &= V_{11} e^{i\phi_{11}} \\ X_{1n} + iY_{1n} e^{i\phi_{1n}} &= V_{1n} e^{i\phi_{1n}} \end{aligned} \tag{5}$$

that are linked to the on crest voltages and phases of the first accelerating cavity (V_{11}, ϕ_{11}) and of the high order harmonic cavity (V_{1n}, ϕ_{1n} with $n = 3$ for the European XFEL case). A loop-procedure ensures that the output values for the required voltages in the injector are below the maximum achievable set-points. This procedure decreases the value of $\delta'''(0)$ in eq. 4 as long as the output values for the injector parameters are outside the limits. In other words we "give up" the correction of part of the third order term of the input distribution because of the limited power achievable in the RF-cavities. Once the setup of the injector has been calculated, it is possible to run fast one-dimensional beam dynamics simulations that use as input the longitudinal phase space distribution at the gun exit produced by ASTRA and transport it up to the $linac_3$ exit using matrix multiplication and including the RF-wakefields of the main linac. We have repeated the injector parameters calculation and the 1D tracking for small variations of the linear term α_1 in order to maximize the local current at the exit of $linac_3$. The setup of the machine corresponding to the maximum local current at the $linac_3$ exit is the final one that will be used for the 3D simulations described in the next section.

2.4. Results

Using the procedure described above for the determination of the machine setup, we have carried out fast 3D start to end simulations using the following codes:

- ASTRA [Floettmann 2011], tracking with space charge in the injector;
- CSRtrack [Dohlus Limberg 2012], tracking including Coherent Synchrotron Radiation (CSR) and with the space charge force option switched off in the laser heater, dogleg and bunch compressors (to significatively reduce the run-time);
- Linear transport matrices multiplication in the linac sections;
- RF-wakefields and longitudinal space charge along the linac sections have been added analytically [Zagorodnov et al. 201

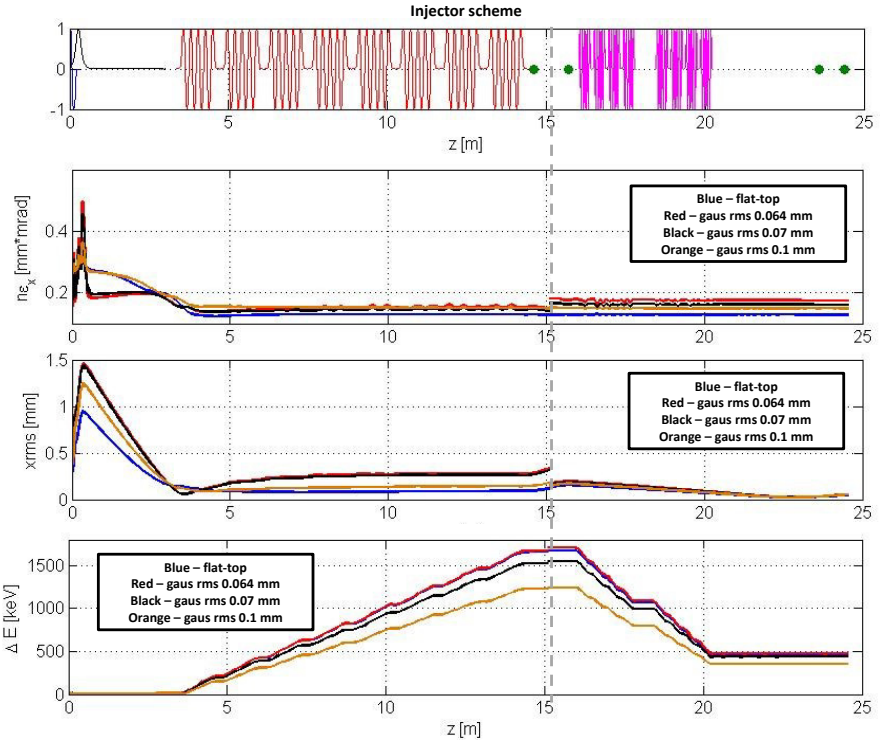

Fig. 4. On top: injector scheme. From right side to left we can see the normalized RF-gun accelerating field and solenoid field (in black), the normalized accelerating field of the first TESLA cavity (red), the normalized electric field of the third harmonic cavity (pink). The green dots correspond to four quadrupoles. In order not to modify the qudrupoles setup for each run, the e-bunch has been artificially matched at 15.1m by rotating its transverse phase space. The same method has been used at other locations along the entire line. Below: normalized emittance, beam envelope and energy spread along the injector for the 4 input distributions.

Table 1. Summary of the partial compression factors for the different input distributions.

Input distr.	*DGL*	BC_0	BC_1	BC_2)
Flat-top	1.3	2.8	7	329
Gaus rms 0.064 mm	1.3	2.1	9.5	259
Gaus rms 0.07 mm	1.3	2.1	9.6	195
Gaus rms 0.1 mm	1.3	2.1	9.6	122

The longitudinal phase space distributions at the linac exit are shown in figure 5. Let us consider first the output corresponding to the 3 longitudinally gaussian beams. We can see a correlation between the initial spotsize and the peak current after compression (Fig. 2). Due to the space charge repulsion, the smallest photo-cathode laser spotsize

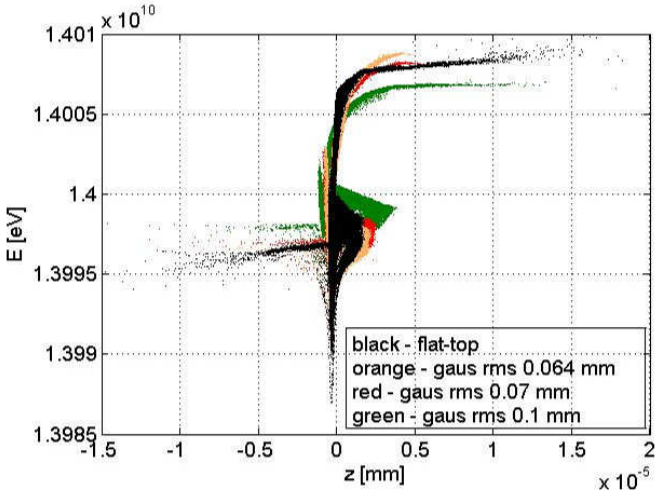

(a)

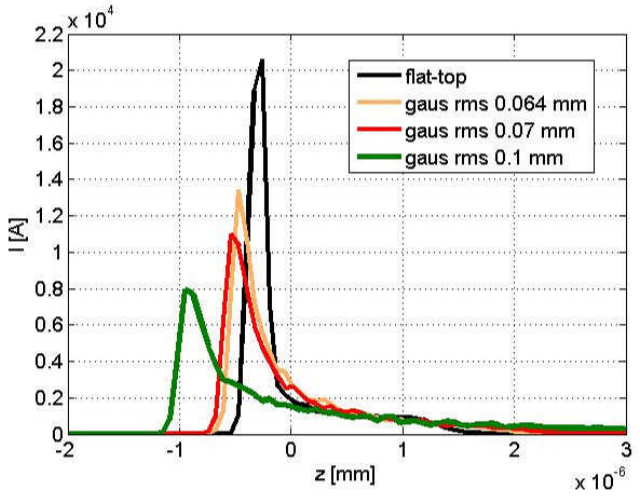

(b)

Fig. 5. Phase space distributions (a) and longitudinal current profiles (b) at the linac exit for the 4 input distributions.

corresponds to the longest electron bunch distribution at the gun exit and to the largest energy spread after the bunch compression. The ”knee”, i.e. the bump on the right side in the lower part of the phase space distributions, in figure 5 (a) is the most interesting part to discuss since it contains the most of the charge (as can be seen in Fig. 6). This feature almost disappears if the CSR effect is not included in the compression and strongly impacts the final peak current. The ”knee” is wider for the shortest electron bunch distribution at the gun exit, that is why this distribution delivers a smaller final peak current. In conclusion we see that, if we want to obtain sub-femtosecond pulses at the linac exit, we can not simply choose the laser setup which delivers the shortest bunch length at the gun exit in order to relax the RF tolerances. Indeed we need to find a compromise by studying the shortest electron bunch at the gun exit which allows to obtain a sufficiently high peak current (or short longitudinal FWHM) after the compression.

The best result has been obtained using the flat-top beam. Its high peak current at the linac exit is not only due to the length of the electron bunch but also to the smaller slice energy spread at the gun exit (see fig. 2). In the Table 1 the projected parameters are summarized.

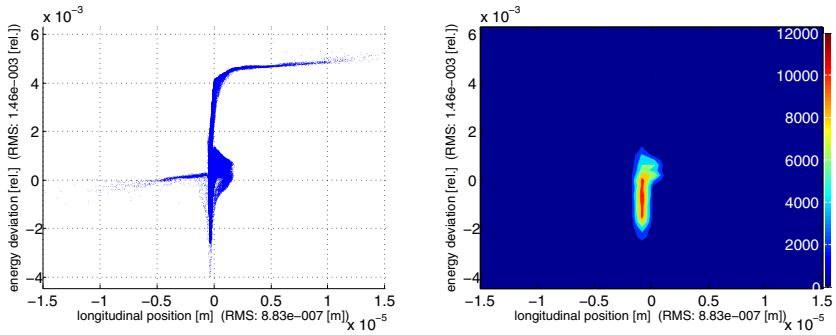

(a) (b)

Fig. 6. Longitudinal phase space distribution of the flat-top beam at the exit of the linac. In (a) the particles coordinates are shown while in (b) the meshed plot highlights the charge density.

Table 2. Summary of the projected parameters at the exit of the linac for the different input distributions.

Input distr.	$n\epsilon_x$ (μ m)	$n\epsilon_y$ (μ m)	Energy spread (*relative*)	FWHM (*fs*)
Flat-top	0.16	1.11	$2.53 * 10^{-4}$	0.74
Gaus rms 0.064 mm	0.224	0.964	$2.67 * 10^{-4}$	0.934
Gaus rms 0.07 mm	0.21	0.92	$2.33 * 10^{-4}$	1.14
Gaus rms 0.1 mm	0.19	0.804	$1.44 * 10^{-4}$	1.44

Finally we would like to show the result that we obtained after tracking the final distributions through the undulator by using the well known Genesis code [Reiche 1999]. We need to emphasize that, in order to simplify the simulations, both the longitudinal space charge field and the undulator wakefields have been neglected for the moment, moreover the transport line between the exit of the linac and the entrance of the first undulator section has not been included. The geometry of the XFEL SASE1 undulator is summarized in the Table 2.

Table 3. Summary of the SASE1 undulator parameters.

Period [mm]	40
Magnetic Field [T]	1.14
K	4.27
E-bunch energy	14
Wavelength [nm]	2.6

We have tracked through the XFEL SASE1 undulator the distribution in fig. 6 and fig. 7 shows the output of Genesis. A single spike, sub-fs pulse, having power of the order of 100 GW has been obtained.

Although these simulations do not yet include many effects that can further spoil the beam, i.e. they do not prove the feasibility of the discussed working points, they pointed out some interesting considerations concerning the link between the initial photo-cathode laser parameters and the shape of the final longitudinal phase space distribution.

3. Conclusions and outlook

A working point for the European XFEL delivering a single spike radiation pulse at 0.26 nm wavelength has been discussed using fast 3D start to end simulations. This configuration presents an e-bunch already fairly short at the gun exit in order to relax the RF tolerances. Full 3D simulations are foreseen using this setup in order to confirm or correct the result. In order to tune the machine settings the full characterization of the electron bunch at the gun exit (in particular the knowledge of its longitudinal phase space distribution) is crucial. Experimental measurements to

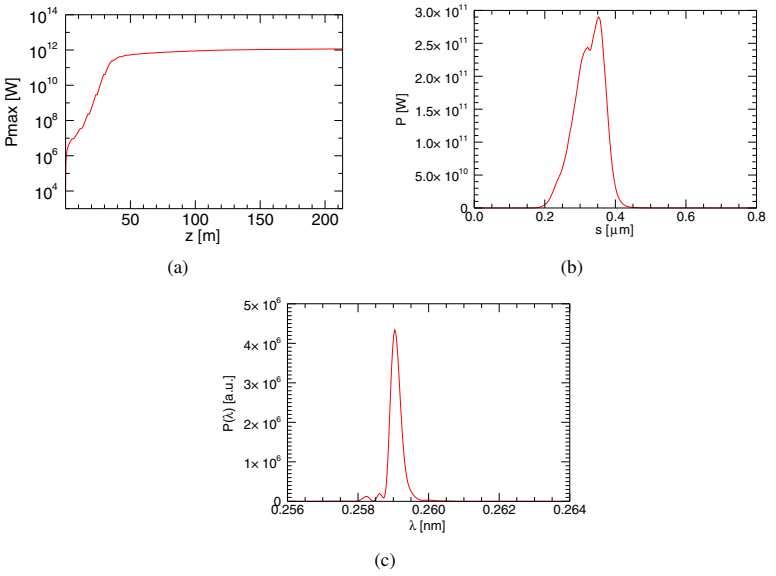

Fig. 7. Maximum power along the undulator (a), temporal profile (b) and power spectrum (c) of the emitted pulse at 38m along the undulator.

characterize the e-bunch properties at the exit of the gun are feasible at the PITZ facility at DESY, Zeuthen site, where the same laser and gun of the XFEL facility are present together with the possibility to fully characterize the electron bunch both in the transverse and longitudinal phase space.

Acknowledgements

The authors would like to thank Martin Dohlus, Sven Reiche, Juliane Roensch Schulenburg and Marie Rehders for profitable clarifications and discussions.

References

[Huang et al. 2007] Z. Huang, K-J. Kim, 2007. Review of x-ray free-electron laser theory. Physical Review Special Topics - Accelerators and Beams 10, 034801.

[Amann et al. 2012] J. Amann et al., 2012. Demonstration of self-seeding in a hard-X-ray free-electron laser. Nature Photonics 6, 693-698.

[Feldhaus et al. 1997] J. Feldhaus et al., 1997. Possible application of X-ray optical elements for reducing the spectral bandwidth of an X-ray SASE FEL. Optics Communications 140, 341-352.

[Giannessi et al. 2011] L. Giannessi et al., 2011. Self-Amplified Spontaneous Emission Free-Electron Laser with an Energy-Chirped Electron Beam and Undulator Tapering. Physical Review Letters 106, 144801.

[Marcus et al. 2012] G. Marcus et al., 2012. Time-domain measurement of a self-amplified spontaneous emission free-electron laser with an energy-chirped electron beam and undulator tapering. Applied Physics Letters 101, 134102.

[Saldin et al 2006] E. Saldin et al., 2006. Self-amplified spontaneous emission FEL with energy-chirped electron beam and its application for generation of attosecond x-ray pulses. Physical Review Special Topics - Accelerators and Beams 9, 050702.

[Thompson et al. 2008] N. R. Thompson, B. W. J. McNeil, 2008. Mode Locking in a Free-Electron Laser Amplifier. Physical Review Letters 100, 203901.

[Dunning et al. 2013] D. J. Dunning et al., 2013. Few-Cycle Pulse Generation in an X-Ray Free-Electron Laser. Physical Review Letters 110, 104801.

[Reiche et al. 2008] S. Reiche et al., 2008. Development of ultra-short pulse, single coherent spike for SASE X-ray FELs. Nuclear Instruments and Methods in Physics Research A 593, 45-48.

[Rosenzweig et al. 2008] J. B. Rosenzweig et al.,2008. Generation of ultra-short. high brightness electron beams for single spike SASE FEL operation. Nuclear Instruments and Methods in Physics Research A 593, 39-44.

[Wang et al. 2011] L. Wang et al., 2011. Optimization for single-spike x-ray FELs at LCLS with a low charge beam. Proceedings of IPAC2011.

[Ding et al. 2009] Y. Ding et al., 2009. Measurements and Simulations of Ultralow Emittance and Ultrashort Electron Beams in the Linac Coherent Light Source. Physical Review Letters 102, 254801.

[Stephan et al. 2010] F. Stephan et al., 2010. Detailed charachterization of electron sources yielding first demonstration of the European X-ray Free-Electron Laser beam quality. Physical Review Special Topics - Accelerators and Beams 13, 020704.

[Krasilnikov et al. 2012] M. Krasilnikov at al., 2012. Experimentally minimized beam emittance from an L-band photoinjector. Physical Review Special Topics - Accelerators and Beams 15, 100701.

[Bonifacio et al. 1994] R. Bonifacio et al., 1994. Spectrum, Temporal Structure, and Fluctuations in a High-Gain Free-Electron Laser Starting from Noise. Physical Review Letters 73, 1.

[Boscolo et al. 2008] I. Boscolo et al., 2008. Single spike operation in SPARC SASE-FEL. Proceedings of EPAC 2008.

[Zagorodnov et al. 2011] I. Zagorodnov, M. Dohlus, 2011. Semianalytical modeling of multistage bunch compression with collective effects. Physical Review Special Topics - Accelerators and Beams 14, 014403.

[Zagorodnov et al. 2010] I. Zagorodnov, 2010. Ultra-short low charge operation at FLASH and the European XFEL. Proceeding of FEL 2010.

[Rehders et al. 2012] M. Rehders et al., 2012. Investigations on the optimum accelerator parameters for the ultra-short bunch operation of the Free-Electron Laser in Hamburg (FLASH). Proceedings of IPAC 2012.

[Will et al. 2008] I. Will, G. Klemz, 2008. Generation of flat-top picosecond pulses by coherent pulse stacking in a multicrystal birefringent filter. Optics Express 16 14922.

[Marchetti et al. 2012] B. Marchetti et al., 2012. Preliminary study of single spike SASE FEL operation at 0.26 nm waavelength for the European XFEL. Proceedings of ICAP 2012.

[Floettmann et al. 2001] K. Flöttmann et al., 2001. Generation of Ultrashort Electron Bunches by cancellation of nonlinear distortions in the longitudinal phase space. TESLA FEL Report 2001-06.

[Floettmann 2011] K. Flöttmann, 2011. ASTRA A Space Charge Tracking Algorithm.

[Dohlus Limberg 2012] M. Dohlus and T. Limberg, 2012. CSRtrack Version 1.2 User's Manual.

[Reiche 1999] S. Reiche, 1999. GENESIS 1.3: a fully 3D time-dependent FEL simulation code. Nuclear Instruments and Methods in Physics Research A 429, 243-248.